NUCL SCI TECH (2018) 29:21
https://doi.org/10.1007/s41365-018-0357-5

New design for multi-crystal data collection at SSRF

Bing Li[1,2] · Sheng Huang[1] · Qiang-Yan Pan[1] · Min-Jun Li[1] · Huan Zhou[1] · Qi-Sheng Wang[1] · Feng Yu[1] · Bo Sun[1] · Jian-Qiao Chen[1,2] · Jian-Hua He[1]

Received: 6 January 2017 / Revised: 12 June 2017 / Accepted: 30 June 2017 / Published online: 29 January 2018

Abstract Data collection with microcrystals at synchrotron radiation facilities is challenging because it is difficult to harvest and locate microcrystals. Moreover, microcrystals are sensitive to radiation damage; thus, typically, a complete data set cannot be obtained with a single microcrystal. Herein, we report a new method for data collection with multiple microcrystals having a crystal size ranging from 1 to 30 μm. This method is suitable for not only low-temperature (100 K) data collection but also room-temperature data collection. Thin Kapton membranes were used to capture multiple crystals simultaneously. The microcrystals were visible under an optical microscope and easily located because the membrane was transparent and sufficiently thin. The film was fixed to a bracket that was prepared using a three-dimensional printer. The bracket was fixed on a magnetic base via screwing and employed by the goniometer system for data collection. Multiple data sets of fatty acid-binding protein 4 (FABP4) and lysozyme microcrystals were collected using this novel designed device. Finally, the structures of protein FABP4 and lysozyme were obtained from these data via the molecule replacement method. The data statistics reveal that this method provides a comparable result to traditional methods such as a nylon loop.

This work was supported by the Strategic Priority Research program of the Chinese Academy of Sciences (No. XDB08030101).

✉ Jian-Hua He
hejianhua@sinap.ac.cn

[1] Shanghai Institute of Applied Physics, Chinese Academy of Sciences, Shanghai 201800, China

[2] University of Chinese Academy of Sciences, Beijing 100049, China

Keywords Kapton membrane · Microcrystals · Multi-crystal data collection · Protein structure

1 Introduction

The structure determination of biological macromolecules with microsize crystal samples is an important and difficult task. Many crystallization methods have been developed, such as the lipid cubic phase (LCP), in which quasi-solid lipidic cubic phases are used for the crystallization of membrane proteins [1]. However, in many cases, the crystallization of proteins is difficult. For example, small crystals can be produced, but making small crystals grow larger with good quality requires extensive exploration, and some microcrystals cannot grow larger. Thus, obtaining high-quality diffraction patterns with microcrystals is a challenge for researchers.

Currently, the nylon loop and microfabricated mount are often used in protein crystallography data collection. However, it is difficult to trap a microcrystal in liquid film, because the nylon rope is soft and flexible. A microfabricated mount for mounting microcrystals was designed by Throne et al. [2]. They wrapped a patterned polyimide film around metal rods, which increased the rigidity of the mount and caused the excess mother liquor to leak out easily. The microfabricated mount is well-suited for mounting single microcrystals. However, small crystals are sensitive to radiation damage, and dozens of crystals are needed to screen and to collect an integral data set. It would be laborious and cost much time to harvest crystals. Some microcrystal-mounting designs can mount multiple crystals simultaneously. For example, the micromesh can mount hundreds of microcrystals. An automated procedure was

developed to locate the crystals mounted on the mesh [3]. Coquelle et al. [4] collected data at room temperature (RT) from crystals sandwiched between two silicon nitride wafers. When micromesh is used to mount microcrystals, especially those having a crystal size below 10 μm, microcrystals are sometimes invisible under the microscope in the beamline station because mother liquor may decrease the transparency of the samples. It is not easy to locate the microcrystals; raster-scanning the micromesh is the recommended technique. Rastering [5] costs a lot of precious experiment time. Nonetheless, the microcrystals are easy to gather together and prone to generating multiple diffractions even with a focused beamline.

To perform the microcrystal experiments, a new crystal-mounting approach, which is based on a chip, was developed for multi-crystal data collection in synchrotron radiation and X-ray free electron laser (XFEL) facilities. Zarrine-Afsar et al. [6] designed a chip that is composed of a silicon mesh and a polyimide film on both sides, preventing the dehydration of the crystals. The chip is engraved with periodic grids, and the crystals are arranged inside the periodic grids. However, the silicon mesh chip is unable to remove excess mother liquid, which may increase the background scattering. Roedig et al. [7] developed a single-crystalline silicon chip with micropores of different size and geometry to avoid the preferred orientation of microcrystals. Excess mother liquor can be removed through the micropores, which reduces the background scattering significantly. Another crystallography chip enables time-resolved and in situ RT crystallography at micro-focused synchrotron beamlines and XFEL sources [8]. In summary, these chip-based methods prearrange the crystals in known locations. Therefore, the hit rate of crystals by the X-ray beam can be increased greatly. However, the fabrication of the chips is expensive, and the ultrathin chips are too fragile to be reused.

As the development of serial crystallography, some methods initially used in XFEL experiments were applied to synchrotron facilities. Crystals are embedded in an LCP viscous mixture or protectant and continuously flow across the beam. Thousands of crystals can be screened in a short time using an LCP jet [9, 10], and this method is also suitable for time-resolved diffraction studies.

Another multiple crystals data-collection method involves utilizing the membrane as the sample holder. Feld et al. [11] employed a low-Z polymer as a sample supporter for XFEL crystallography experiments. Baxter et al. [12] developed a goniometer-based sample delivery method that used a high-density sample grid as a scaffold for both crystal growth and diffraction experiments. The grid scaffold is made of polycarbonate film with rows of laser-cut pores. To hold the samples, one face of the grid is covered with 5-μm-thick polycarbonate film. Large crystals are visible and easily located. However, crystals smaller than 30 μm cannot be visualized, and a rastering strategy was applied to scan the pores one by one. Table 1 briefly summarizes the various methods used for microcrystal sample delivery at synchrotron radiation facilities.

In this paper, we present a multiple-microcrystal sample delivery approach for the Shanghai Synchrotron Radiation Facility (SSRF) BL17U1 macromolecular beamline. Microcrystal samples are deposited on a 12.5-μm-thick Kapton film, which enables efficient crystal loading and allows microcrystals with 1–30 μm in size to be easily located. This approach works well at the cryotemperature and RT. We collect limited diffraction patterns per crystal according to their tolerance to the radiation damage. Hundreds of microcrystals can be dispersed on the membrane arbitrarily and separately. The excess mother liquor can be removed via a special capillary with a small diameter. Small crystals larger than 10 μm are visible under the microscope, and we do not need to raster the membrane to locate them. Moreover, the bracket, which was used to support the thin Kapton film, was manufactured using a photosensitive resin laser three-dimensional printer (Form1+). It was fixed on a magnetic base via screwing and employed on the goniometer system for data collection. The sample holder was mounted and dismounted using robotic sample changers during operation at the cryotemperature.

2 Methods and materials

2.1 Design and fabrication

The main purposes of the crystal sample mounting device are to collect low-background diffraction data from multiple microcrystals with a crystal size larger than 10 μm at cryogenic temperatures (100 K) or RT and to increase the hit rate of the X-ray onto the crystal. In our design (Fig. 1), a polyimide film (Kapton film) 12.5 μm thick is used as the loading material to achieve these goals. When the photon energy is in the range of 9–15 keV, the X-ray transmission ratio of the Kapton film is $> 99\%$ (http://henke.lbl.gov/optical_constants/filter2.html).

The film is suitable for crystals larger than 10 μm because they can be easily located under a microscope, as shown in Fig. 1d. Considering the diameter of the nitrogen cryostream and the size of the inline camera visual window, a membrane with dimensions of 2×4 mm^2 is used. The size of the membrane supporting bracket is determined by the size of the membrane positioning range, which is given by the goniometer. At the edge of the bracket, there is a rectangular groove with dimensions of $1.5 \times 1.2 \times 0.6$ mm^3, as shown in Fig. 1a. The

Table 1 Microcrystal sample delivery methods used at synchrotron radiation facilities

Method	Optimum crystal size (μm)	Goniometer compatible	Centering	Mount one or multiple crystals at a time	Temperature	Single or multiple images per crystal
Microfabricated mount	~ 10	Yes	Raster/crystal visible	Single	100 K	Multiple
Micromesh	> 10	Yes	Raster	Multiple	100 K	Multiple
Crystals sandwiched	No limitation	Yes	Raster	Multiple	RT	Single
Fixed target matrix chip	< 4	Yes/no	Crystals located at defined positions	Multiple	RT 100 K	Multiple/single
Jet	Depends on diameter of nozzle	No	Inject sample liquid to X-ray beam	Multiple	RT	Single
Membrane	> 1 μm	Yes	Visible/raster	Multiple	RT/100 K	Multiple/single

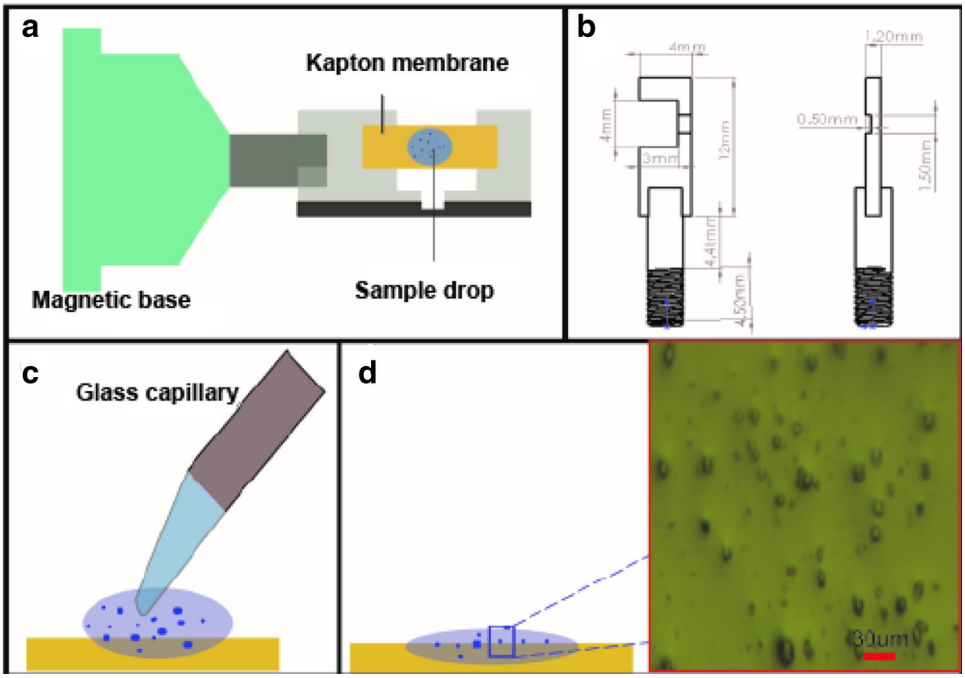

Fig. 1 (Color online) **a** Schematic of the crystal sample mounting device. **b** Specific size of the membrane supporting bracket. **c** Glass capillary with a tip less than 100 μm in diameter was used to remove excess protection liquid. **d** After the removal of the excess protection liquid, the crystals were kept in a thin layer of liquid, and every crystal was dispersed

rectangular groove helps to center the crystals. Drawings of the membrane support bracket and detailed dimensions are shown in Fig. 1b. The membrane is fixed on the surface of the support bracket with SuperGlue (Hampton Research Co.).

Microcrystals were transferred to the membrane easily via pipette from the crystallization vessels. A capillary with a tip diameter of < 100 μm was used to suck out excess protection liquor, which helped to keep the crystals in a thin layer of protection liquor. The background scattering from the protection solution was significantly reduced. Data collection was performed at low temperatures, which prevented the crystals from drying. Working at low temperatures reduced the radiation damage, especially for the microcrystals.

2.2 Crystal preparation

Chicken egg white lysozyme microcrystals larger than 10 μm and needle-like FABP4 crystals with dimensions of 10 μm × 150 μm were used as test samples.

The chicken egg white lysozyme microcrystals were obtained via a seeding method. Crystal seeds were obtained from large lysozyme crystal fragments. The crystallization drops comprised 1 μL of a protein sample (20 mg mL^{-1} lysozyme) and 1 μL of a reservoir solution (mixture of 0.2 M citric acid and 0.2 M sodium acetate at a 1:1 ratio,

8% (w/v) NaCl). Then, 0.2 μL of a seeding crystal solution was added to the crystallization drops as seeds. After 4 h, lysozyme microcrystals smaller than 30 μm were obtained.

Crystals of FABP4 were grown using the hanging-drop vapor-diffusion method. The crystallization drops comprised 1 μL of a protein sample (5 mg mL^{-1} FABP4 in 20 mM Tris-HCl, pH = 7.5, 50 mM NaCl buffer) and 1 μL of a reservoir solution (1.6 M sodium citrate pH 6.5). Crystals appeared after 3–4 days of incubation at 291 K and exhibited a rod-like shape with a size of 10 μm × 150 μm.

2.3 Sample loading

First, 2–4 μL of cryoprotectant (30% glycerol and 70% reservoir solution) was deposited on the membrane using a pipette. When performing the experiments at RT, we added 2–4 μL of mother liquid on the membrane. Second, a micromesh loop was used to harvest 50–100 crystals and then to transfer the crystals into a drop of cryoprotectant or mother liquid. The micromesh loop was slightly stirred to make the crystals well-dispersed in the protectant. Because a micromesh loop can harvest dozens of crystals at a time, it only takes a few seconds to mount hundreds of crystals on the membrane. Third, a glass capillary with a tip diameter less than 100 μm was used to remove excess liquid. Removing excess protectant helps to reduce background scattering and disperse crystals with less overlapping. For collecting data at the cryotemperature, the mounted samples were flash frozen in liquid nitrogen for further diffraction experiments. If we collect data at RT, we need another piece of Kapton membrane to seal crystal sample to protect it from dehydration.

2.4 Data collection

Data collection was performed at the SSRF macromolecular crystallography (MX) beamline BL17U1. Diffraction experiments for lysozyme and FABP4 were performed using a focused beam of size (full width at half maximum) of 67 × 23 μm^2 (H × V) at an energy of 12.6 keV. The photon flux at the sample point was 3.8×10^{12} phs/s [13].

The diffraction data were collected at 100 K under the nitrogen stream or at RT. The sample supporting bracket was mounted on a goniometer manually to make the membrane surface roughly perpendicular to the X-ray beam. Manual mounting leads to an error of ± 5°, causing the samples to appear blurry. Further steps are necessary to bring the samples to the beam and make the crystals appear distinct. The sample can also be mounted using robotic sample changers while performing experiments at the cryotemperature. The procedures for centering the crystals are described as follows. Rotation by + 90° (or by − 90°), selecting the membrane edge, and rotating back allow us to bring the crystals into the beam. If a rotation by + 90° or back rotation does not lead to a clear view of the crystals, we must rotate in the opposite direction. Under normal conditions, we may observe crystals clearly or slightly blurry via rotation. If crystal image is slightly blurry, we can randomly adjust the sample position parameters (sample X and sample Y) until the image becomes distinct. In this way, crystals can be seen clearly, and we can locate a crystal by clicking it.

Sample radiation damage cannot be drastically reduced in X-ray diffraction experiments, which always leads to a decay of the diffraction intensity. Microcrystals are very sensitive to radiation damage, which is the dominant reason for the failure of obtaining the phase from sulfur single-wavelength anomalous dispersion data in the structure solution. When the data collection should be stopped and how many images should be collected are determined by the dose limit, which was proposed by Owen et al. [14]. According to the analysis of the electron density in terms of the number of damaged residues, along with other data-quality indicators, Owen et al. found that by the time $D_{1/2}$ (dose required to reduce the diffraction intensity by half) is reached, the integrity of the biological information is compromised. Consequently, they suggest an upper dose limit of 30 MGy. RADDOSE-3D [15] is used to ensure that the absorbed doses are within the Henderson limit. With the setting of the lysozyme crystal dimensions ($10 \times 10 \times 10$ μm^3), as well as the beam and experimental parameters of BL17U1, the RADDOSE-3D results show that for collecting 30 diffraction images with a rotation increment of 1°, the average radiation dose to the exposed region is 25.0 MGy, which is below the Henderson limit of 30 MGy. As a result, 30 diffraction images can be obtained without compromising the biological information from the given crystals 10 μm in size. Considering the membrane flat hindrance and radiation damage, 10–30 diffraction images can be collected per crystal in our experiments. For collecting 40 diffraction images with a rotation increment of 1° of FABP4 crystals with crystal dimensions of $10 \times 100 \times 10$ μm^3, the average radiation dose of exposed region is 21.1 MGy; thus, the crystals are weakly exposed.

2.5 Data processing and analysis

As there are dozens of crystals on the membrane, crystal screening and data collection were performed from the left side of the membrane to the right side and from the top to the bottom, guided by the inline camera. After the crystals were screened on the membrane, 22 FABP4 crystals were selected for data collection with an oscillation angle of

approximately 40°. The data sets were integrated and scaled by using HKL2000 [16]. The multiple integrated data sets were merged and scaled together using Scalepack. Integrating every data set with HKL2000 led to 16 data sets that were considered acceptable, i.e. having a higher resolution and positional and partiality values of $\chi^2 < 2$. Overall, 374 images were merged into a complete data set. The structure of FABP4 was solved via molecular replacement [17] using PDB 4nns as the searching model, refined with the Refmac program [18], and manually built with Coot [19].

For lysozyme crystals, the crystal size is between 10 and 20 μm. According to the results of RADDOSE-3D, 30 diffraction images were collected for the 10-μm crystals. After the lysozyme crystals were screened, 27 crystals were selected to collect 27 data sets of 390 images. After the diffraction data were indexed, the intensities were integrated, and the data were merged using HKL2000. The structure of the lysozymes was solved via molecular replacement using PDB 5l9j as the searching model and refined with the Refmac program in CCP4 [18, 20]. The lysozyme protein structure was manually built with Coot [19].

3 Result and discussion

3.1 Background scattering from membrane

Resolution is an important parameter for evaluating diffraction data. The highest-resolution shells were determined using the following criteria: signal-to-noise ratio $\langle I/\sigma(I)\rangle > 2$, redundancy > 2, completeness $> 90\%$, and $R_{\text{merge}} > 50\%$.

Background scattering affects the $\langle I/\sigma(I)\rangle$ ratio of data. $\langle I/\sigma(I)\rangle$ is one of the criteria for defining the resolution cutoff. The background scattering in this experiment was mainly caused by the protection solvent and Kapton films. The polyimide film with a thickness of 12.5 μm was almost transparent to X-rays having energies between 9 and 15 keV (transmission $> 99\%$). To measure the background contribution of the membrane, two diffraction images were collected, with and without the membrane. A comparison of the background noise in the same position of the two diffraction images is shown in Fig. 2a, b. The value of the background noise with and without the membrane has almost no difference, which means that the membrane sample holder did not contribute to the background scattering. To further reduce the background scattering, the excess cryoprotectant buffer was removed using a glass capillary. To validate the extremely low-background scattering from the membrane sample holder, two complete data sets of FABP4—one with a nylon loop and another with a Kapton membrane as the sample holder—were collected. The results of the signal-to-noise ratio in every resolution shell of the two data sets are shown in Fig. 2c, d. The signal-to-noise ratio at the highest-resolution shell obtained using the membrane sample holder is larger than that from the loop. However, at the lowest-resolution shell, the signal-to-noise ratio from the loop is higher than that with the membrane. Because the difference is not obvious, we conclude that the background scattering from the membrane sample holder can be neglected.

3.2 Structure determination with large crystals

To verify the suitability of the membrane sample holder for X-ray crystallography experiments, FABP4 crystals larger than 40 μm were chosen as test samples. Data collection was performed at the SSRF MX beamline BL17U1 at 100 K. Crystals can be clearly seen on the membrane and easily located under the inline camera. After the crystals were screened on the membrane, 22 crystals were selected for data collection. Less than 40 images spanning an oscillation angle of 40° were collected from each crystal, owing to membrane flat hindrance. The diffraction data were processed with HKL2000 [16]. Some images or data sets with poor diffraction quality were deleted or extruded manually and not used for further processing. Finally, 16 data sets with 374 images were merged into a complete data set. According to the aforementioned resolution cutoff criteria, the highest resolution of the multi-crystal data set was 1.55 Å.

A data set was collected with a single FABP4 crystal, which was grown in the same drop as those for the membrane method, using the nylon loop. Finally, 270 images were collected with 1 s per image and a rotation increment of 1°. Data reduction, structure solving, and refinement were performed using the same method that was used for multiple data sets. A comparison of the data collection and refinement statistics for these two methods is presented in Table 2.

In this experiment, a Kapton membrane was successfully utilized to mount dozens of crystals simultaneously, and multiple data sets were collected from different crystals. After merging multiple data sets, a complete data set can be obtained, and the structure can be solved. Because more diffraction images were used to merge to one data set than a single-crystal data set used, the redundancy of multiple crystals in some shell of resolution is higher than that of a single crystal. We can conclude that even crystals on membrane have a preferred orientation, which can be ignored because the redundancy is high and does not affect the resolution cutoff. The average signal-to-noise ratio of multiple crystals is 33.5, which is slightly smaller than the value of 38.5 for a single crystal, as shown in Table 2. This

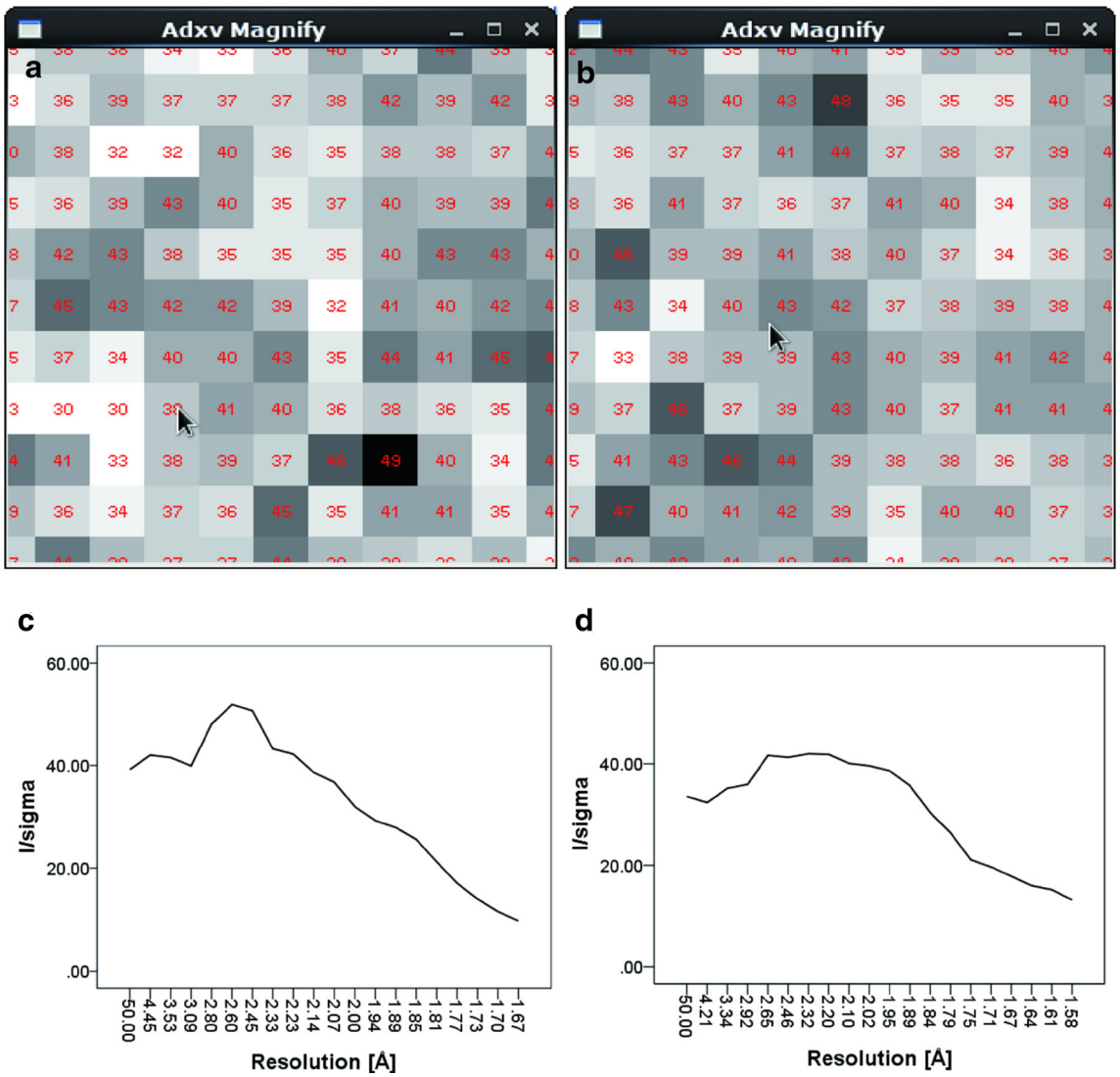

Fig. 2 (Color online) Background noise of air (**a**) and the membrane (**b**) derived from the same coordinate point of the two diffraction patterns. **c** Signal-to-noise ratio in every resolution shell of the diffraction data obtained from a single FABP4 crystal in the nylon loop. **d** Signal-to-noise ratio in every resolution shell of the diffraction data obtained from multiple FABP4 crystals in the membrane

may be because the signal-to-noise ratio usually decreases with the decrease of the resolution. The resolution of 1.55 Å achieved with multiple crystals is higher than the resolution of 1.64 Å achieved with a single crystal. If the size of the FABP4 crystals is 100 µm, the radiation damage has little influence on the diffracted intensity. The quality of the data obtained via the membrane method is as good as that of the data obtained with the nylon loop. To verify that the device can also be employed for data collection at RT, we use dozens of FABP4 crystals as test samples. The detailed data collection and refinement statistics are shown in Table 2. In conclusion, the membrane mounting method is suitable for data collection and structure solving of proteins for multiple crystals and can also be used for RT data collection.

3.3 Structure determination with microcrystals

To verify the usefulness of the membrane mounting method for microcrystal data collection, lysozyme crystals smaller than 20 µm were chosen as samples. Microcrystals are very sensitive to radiation damage. According to the calculated results from RADOSE-3D, less than 30 images with 1 s per image and a rotation increment of 1° were collected for each crystal. Efficiently locating microcrystals is difficult, and rastering is a common method to accomplish this. A Kapton membrane 12.5 µm thick is transparent enough and makes the microcrystals easily to be figured out on its surface under the inline camera (Fig. 1d). Using the aforementioned method, hundreds of microcrystals were sprayed on the membrane within 2 min.

Table 2 Data collection and refinement statistics of FABP4 using a nylon loop and a membrane as the sample holder for data collection. The data collection for multiple crystals was performed at a low temperature (100 K) and RT, respectively

	Nylon loop (100 K)	Membrane (100 K)	Membrane (RT)
Data collection			
Dominant size in sample (μm)	100	100	100
Number of data sets	1	16	23
Number of images	270	374	314
Space group	$P2_12_12_1$	$P2_12_12_1$	$P2_12_12_1$
Unit cell			
a, *b*, *c* (Å)	32.3, 53.7, 75.0	32.2, 53.4, 74.9	32.6, 53.6, 75.7
α, *β*, *γ* (°)	90, 90, 90	90, 90, 90	90, 90, 90
Energy (keV)	12.6	12.6	12.6
Resolution range (Å)	43.68–1.64	43.47–1.55	43.73–1.76
Number of unique reflections	16,692	19,565	13,751
Completeness (%)	99.1 (92.7)[a]	97.8 (91.6)	93.0 (94.6)
R_{merge} (%)[b]	7.2 (32.6)	6.2 (11.0)	17.7 (33.4)
$\langle I/\sigma(I)\rangle$	38.4 (9.8)	33.5 (13.1)	56.73 (27.35)
Redundancy	11.3 (5.0)	9.8 (6.0)	12.2 (11.9)
Refinement			
R_{work}/R_{free}	0.18/0.20	0.18/0.23	0.18/0.23
Number of non-hydrogen atoms	1158	1169	1084
Number of ions	0	0	0
Number of water	113	124	39
B-factors[2]			
Overall	15.45	13.0	23.9
Protein	14.3	11.9	23.7
Ion	0	0	0
Water	26.01	21.92	28.8
R.m.s. deviations			
Bond lengths (Å)	0.02	0.02	0.02
Bond angle (°)	2.13	2.34	2.06
Ramachandran plot (%)			
Most favored	96.97	96.97	98.48
Allowed	3.03	3.03	1.52
Disallowed	0.0	0.0	0.0

[a]The values in parentheses correspond to the outermost shell

[b]$R_{merge} = \sum_{hkl}\sum_i |I_i(hkl) - \langle I(hkl)\rangle| / \sum_{hkl}\sum_i I_i(hkl)$,where $\langle I(hkl)\rangle$ is the mean intensity of a set of equivalent reflections

After the crystals were screened one by one, 27 data sets were collected, and 20 data sets were merged into a complete data set according to the data quality. As a control, a microfabricated mount [7] was used to collect data for a single microcrystal. A total of 201 diffraction images were collected, with a rotation increment of 1°. The data-quality statistics for a single microcrystal and multiple microcrystals are presented in Table 3. Compared with the data collected from a single microcrystal, the data collected from multiple crystals exhibit a better signal-to-noise ratio and resolution, as shown in Table 3. This may be because using the Kapton membrane led to low-background noise and the excess liquid was removed, which helped to reduce the background scattering. In summary, the Kapton membrane-based crystal-mounting method is suitable for microcrystal data collection.

4 Conclusion

We developed a new device to mount crystals—particularly microcrystals—for MX diffraction experiments. The experiments can be conducted at RT or the cryotemperature. Using a Kapton membrane, hundreds of crystals can be mounted on a goniometer simultaneously. Compared with the regular data-collection method for a single crystal, a large number of crystals on the Kapton membrane can be continuously screened. We use a limited number of crystals

Table 3 Data-collection statistics for a single lysozyme microcrystal smaller than 20 μm mounted using microfabricated mounts, and for multiple lysozyme microcrystals mounted using a membrane

	Microfabricated mounts	Membrane
Data collection		
Dominant size in sample (μm)	< 20	< 20
Number of data sets	1	20
Number of images	201	390
Space group	$P4_32_12_1$	$P4_32_12_1$
Unit cell		
a, *b*, *c* (Å)	78.5, 78.5, 37.1	78.9, 78.9, 37.1
α, β, γ (°)	90, 90, 90	90, 90, 90
Energy (keV)	12.6	12.6
Resolution range (Å)	55.0–1.49	55.8–1.34
Number of unique reflections	22,740	27,073
Completeness (%)	99.9 (100)[a]	98.8 (95.4)
R_{merge} (%)[b]	12.5 (35.6)	10 (32.2)
$\langle I/\sigma(I)\rangle$	18.53 (11.25)	27.89 (3.55)
Redundancy	13.3 (14.5)	19.8 (2.8)
Refinement		
R_{work}/R_{free}	0.19/0.21	0.18/0.20
Number of non-hydrogen atoms	1099	1108
Number of ions	0	0
Number of water	98	107
B-factors[2]		
Overall	14.7	16.4
Protein	14.0	15.7
Ion	0	0
Water	22.2	23.1
R.m.s. deviations		
Bond lengths (Å)	0.02	0.02
Bond angle (°)	2.38	1.90
Ramachandran plot (%)		
Most favored	96.85	96.85
Allowed	3.15	3.15
Disallowed	0.0	0.0

[a]The values in parentheses correspond to the outermost shell

[b]$R_{merge} = \sum_{hkl}\sum_i|I_i(hkl) - \langle I(hkl)\rangle|/\sum_{hkl}\sum_i I_i(hkl)$,where $\langle I(hkl)\rangle$ is the mean intensity of a set of equivalent reflections

(< 50) to collect a complete data set, and the radiation damage for each data set is within dose limits. This allows the structure determination of radiation-sensitive crystals. The method for coating the crystals on the membrane saves time in sample preparation, and the excess protectant can be removed within 10 min. The membrane is transparent, and the microcrystals are easily located. In the experiments, the Kapton membrane has a high transmission rate for X-rays, and the excess protectant is removed; thus, the resulting background scattering is considered negligible. Applying the Kapton membrane to mount crystals has proven to be an effective technique for microcrystal data collection.

Acknowledgements We gratefully acknowledge the advice of Rui Wang regarding the processing of data. We thank the staff of beamline BL17U1, who helped us conduct our experiments smoothly. Dr. Ye-Chun Xu is gratefully acknowledged for her assistance with the FABP4 protein samples.

References

1. E.M. Landau, J.P. Rosenbusch, Lipidic cubic phases: a novel concept for the crystallization of membrane proteins. Proc. Natl. Acad. Sci. USA **93**, 14532–14535 (1996). https://doi.org/10.1073/pnas.93.25.14532
2. R. Thorne, Z. Stum, J. Kmetko et al., Microfabricated mounts for high-throughput macromolecular cryocrystallography. J. Appl.

Crystallogr. **36**, 1455–1460 (2003). https://doi.org/10.1107/S0021889803018375
3. U. Zander, G. Bourenkov, A.N. Popov et al., MeshAndCollect: an automated multi-crystal data-collection workflow for synchrotron macromolecular crystallography beamlines. Acta Crystallogr. D Biol. Crystallogr. **71**, 2328–2343 (2015). https://doi.org/10.1107/S1399004715017927
4. N. Coquelle, A.S. Brewster, U. Kapp et al., Raster-scanning serial protein crystallography using micro- and nano-focused synchrotron beams. Acta Crystallogr. D Biol. Crystallogr. **71**(5), 1184–1196 (2015). https://doi.org/10.1107/S1399004715004514
5. V. Cherezov, M.A. Hanson, M.T. Griffith et al., Rastering strategy for screening and centring of microcrystal samples of human membrane proteins with a sub-10 microm size X-ray synchrotron beam. J. R. Soc. Interface **6**(Suppl 5), S587–S597 (2009). https://doi.org/10.1098/rsif.2009.0142.focus
6. A. Zarrine-Afsar, T.R. Barends, C. Muller et al., Crystallography on a chip. Acta Crystallogr. D Biol. Crystallogr. **68**, 321–323 (2012). https://doi.org/10.1107/S0907444911055296
7. P. Roedig, I. Vartiainen, R. Duman et al., A micro-patterned silicon chip as sample holder for macromolecular crystallography experiments with minimal background scattering. Sci. Rep. **5**, 10451 (2015). https://doi.org/10.1038/srep10451
8. C. Mueller, A. Marx, S.W. Epp et al., Fixed target matrix for femtosecond time-resolved and in situ serial micro-crystallography. Struct. Dyn. **2**, 054302 (2015). https://doi.org/10.1063/1.4928706
9. U. Weierstall, D. James, C. Wang et al., Lipidic cubic phase injector facilitates membrane protein serial femtosecond crystallography. Nat. Commun. **5**, 3309 (2014). https://doi.org/10.1038/ncomms430
10. P. Nogly, D. James, D. Wang et al., Lipidic cubic phase serial millisecond crystallography using synchrotron radiation. IUCrJ **2**, 168–176 (2015). https://doi.org/10.1107/S2052252514026487
11. G.K. Feld, M. Heymann, W.H. Benner et al., Low-Z polymer sample supports for fixed-target serial femtosecond X-ray crystallography. J. Appl. Crystallogr. **48**, 1072–1079 (2015). https://doi.org/10.1107/s1600576715010493
12. E.L. Baxter, L. Aguila, R. Alonso-Mori et al., High-density grids for efficient data collection from multiple crystals. Acta Crystallogr. D Struct. Biol. **72**, 2–11 (2016). https://doi.org/10.1107/S2059798315020847
13. Q.S. Wang, F. Yu, S. Huang et al., The macromolecular crystallography beamline of SSRF. Nucl. Sci. Tech. **26**, 010102 (2016). https://doi.org/10.13538/j.1001-8042/nst.26.010102
14. R.L. Owen, E. Rudino-Pinera, E.F. Garman, Experimental determination of the radiation dose limit for cryocooled protein crystals. Proc. Natl. Acad. Sci. USA **103**, 4912–4917 (2006). https://doi.org/10.1073/pnas.0600973103
15. O.B. Zeldin, M. Gerstel, E.F. Garman, RADDOSE-3D: time- and space-resolved modelling of dose in macromolecular crystallography. J. Appl. Crystallogr. **46**, 1225–1230 (2013). https://doi.org/10.1107/s0021889813011461
16. Z. Otwinowski, W. Minor, Processing of X-ray diffraction data collected in oscillation mode. Methods Enzymol **276**, 307–326 (1997). https://doi.org/10.1016/S0076-6879(97)76066-X
17. A. Vagin, A. Teplyakov, MOLREP: an automated program for molecular replacement. J. Appl. Crystallogr. **30**, 1022–1025 (1997). https://doi.org/10.1107/S0021889897006766
18. G.N. Murshudov, P. Skubak, A.A. Lebedev et al., REFMAC5 for the refinement of macromolecular crystal structures. Acta Crystallogr. D Biol. Crystallogr. **67**, 355–367 (2011). https://doi.org/10.1107/S0907444911001314
19. P. Emsley, K. Cowtan, Coot: model-building tools for molecular graphics. Acta Crystallogr. D Biol. Crystallogr. **60**, 2126–2132 (2004). https://doi.org/10.1107/S0907444904019158
20. C.P. Collaborative, The CCP4 suite: programs for protein crystallography. Acta Crystallogr. D Biol. Crystallogr. **50**, 760 (1994). https://doi.org/10.1107/S0907444994003112